

---

# DENOISING DIFFUSION PROBABILISTIC MODEL - APPLICATION TO SATELLITE AND HANDWRITTEN DIGITS IMAGE GENERATION

---

FYS5429 - PROJECT2

 **Romain Corseri\***

University of Oslo  
romain.corseri@gmail.com

June 4, 2024

## ABSTRACT

This report investigates the potential of denoising diffusion probabilistic models for image generation, with a focus on optical satellite images. We adapt a PyTorch implementation of a diffusion model for image resolution enhancement to generate realistic satellite images and use the MNIST dataset to benchmark our model architecture. Our experiments consist in testing the amount and type of training images to demonstrate the effectiveness of diffusion models in generating high-quality images. The results highlight the striking potential of diffusion model for change detection in satellite imagery. Despite the computational challenges and tractability, we emphasize the increasing value of pre-trained "foundations" models for democratizing access to advanced generative capabilities and suggest further research into practical applications in remote sensing and Earth observation.

## 1 Introduction

In recent years, deep generative models have gained considerable attention with striking image generation capability and the advent of large language models (Jonathan Ho [2020], Kingma; and Welling [2019], Nichol [2021], Goodfellow [2014]). Many researchers believe that generative models have the potential to change our research methods and represent a new scientific revolution (Kuhn [1962]). In this work, we investigate the potential of denoising diffusion probabilistic models for image generation. In particular, we are interested in satellite image generation. Vast amounts of optical satellite images are now openly available online and thereby represent a large corpus of training data for diffusion models. There are countless applications in the field of change detection from satellite image analysis. Detection change using synthesized images from diffusion model (Patel [2022]) could contribute from disaster mitigation, climate-change monitoring to military surveillance. In this work, we adapt a PyTorch implementation of diffusion model for image resolution enhancement (Chitwan et al. [2021]) to satellite image generation and we also use MNIST handwritten digits images to benchmark our model architecture requiring less training images and GPU-cycles. Finally, we discuss diffusion model performance, tractability and the potential of open-access large pre-trained "foundations" diffusion model for scientific purposes.

## 2 Denoising diffusion probabilistic model

Denoising diffusion probabilistic models, often simply called diffusion models, belong to the class of probabilistic generative models comprising generative adversarial networks, variational auto-encoders, energy-based model amongst others (Goodfellow [2014], Kingma; and Welling [2019], Luo [2022]). More specifically, diffusion models are hierarchical variational auto-encoders that fulfill three conditions:

- The latent spaces dimension is equal to the input data dimension

---

\*Use footnote for providing further information about author (webpage, alternative address)—*not* for acknowledging funding agencies.

- The encoder is predefined as a linear Gaussian model
- The parameters of the Gaussian model of the encoder vary over time steps so the image at the final time step  $t = T$  is completely contaminated by Gaussian noise (Fig. 1a).

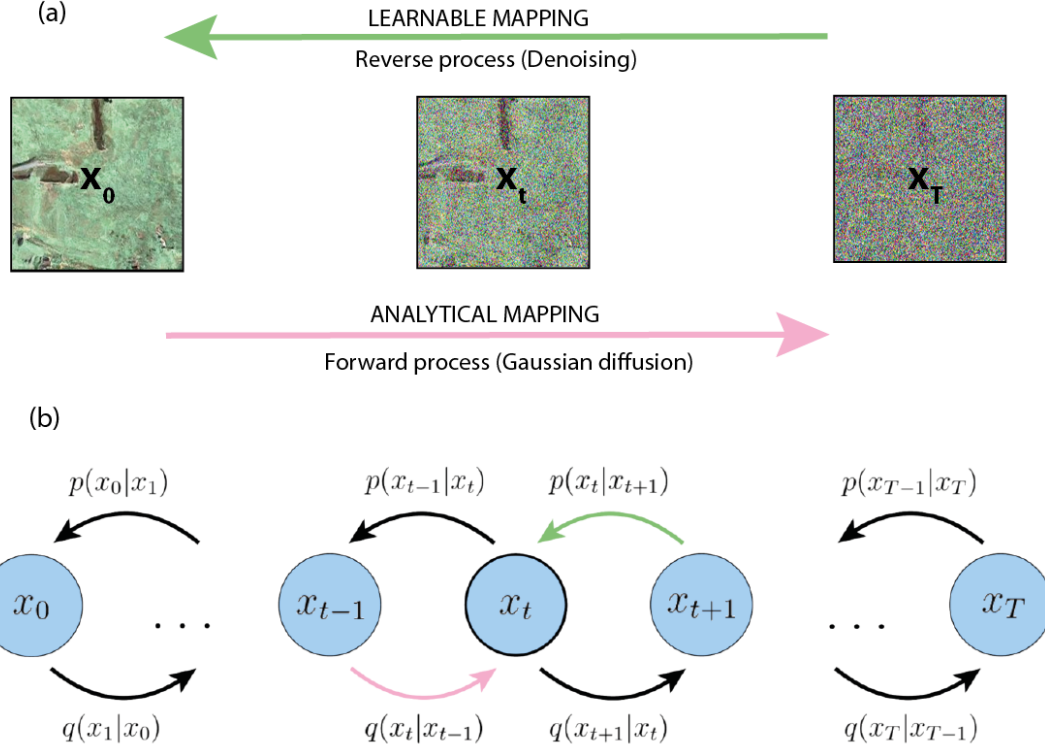


Figure 1: a) Conceptual depiction of denoising diffusion model b) Probability distributions for both forward and reverse Markovian chains in a typical diffusion model for unconditional image generation (figure modified from Luo [2022])

In the two following subsections, we will go through the mathematical basics of diffusion models. We will spell out the most important equations, starting from the forward gaussian diffusion modelling and finishing with the reverse learnable denoising process (Fig. 1a). The section is adapted from Luo [2022], Jonathan Ho [2020] where the mathematical proofs are fully developed.

## 2.1 Gaussian diffusion process

An important property of diffusion models is that the forward process (also called encoder using VAE terminology) can be expressed analytically as a sampling on a Markov chain that gradually adds gaussian noise to the initial images following a variance scheduler  $\beta_1, \dots, \beta_t, \dots, \beta_T$  until the image is purely gaussian noise. In our case,  $\beta_t$  and  $t$  the number of time steps are hyperparameters. Then, at an arbitrary time steps  $t$ , the sampling process of an image  $\mathbf{x}_t$  (Fig. 1) is expressed as:

$$q(\mathbf{x}_t|\mathbf{x}_0) = \mathcal{N}(\mathbf{x}_t; \sqrt{\alpha_t}\mathbf{x}_0, (1 - \alpha_t)\mathbf{I}) \quad (1)$$

$$\text{with } \alpha_t = 1 - \beta_t \text{ and } \overline{\alpha_t} = \prod_{i=1}^t \alpha_i \quad (2)$$

## 2.2 Reversing diffusion by optimizing the denoising model

The denoising model takes as input the noisy image  $\mathbf{x}_t$  and output a denoised image  $\mathbf{x}_{t-1}$  (Fig. 1b). It can proven that, under some assumption, the denoising step from time  $t$  to  $t - 1$  can be expressed as:

$$q(\mathbf{x}_{t-1}|\mathbf{x}_t, \mathbf{x}_0) = \mathcal{N}(\mathbf{x}_{t-1}; \tilde{\mu}_t(\mathbf{x}_t, \mathbf{x}_0), \tilde{\beta}_t\mathbf{I}) \quad (3)$$

$$\text{where } \tilde{\mu}_t(\mathbf{x}_t, \mathbf{x}_0) = \frac{\sqrt{\alpha_{t-1}}\beta_t}{1-\bar{\alpha}_t} \mathbf{x}_0 + \frac{\sqrt{\alpha_t}(1-\bar{\alpha}_{t-1})}{1-\bar{\alpha}_t} \mathbf{x}_t \text{ and } \tilde{\beta}_t = \frac{1-\bar{\alpha}_{t-1}}{1-\bar{\alpha}_t} \beta_t. \quad (4)$$

Given that the ultimate goal of the diffusion model is to learn a Markov chain  $p_\theta(\mathbf{x}_0)$  that aims to mimic the original data distribution (i.e. the original image  $p(\mathbf{x}_0)$ ) by maximizing the Evidence Lower Bound (ELBO). The Kullback–Leibler (KL) divergence  $\mathcal{D}_{KL}$  measures the dissimilarity between two probability distributions. Here, the equivalent ELBO maximisation problem is equivalent to minimizing  $\mathcal{D}_{KL}$  between the learned probability distribution  $p_\theta(\mathbf{x}_{t-1}|\mathbf{x}_t)$  and the ground-truth denoising transition step  $q(\mathbf{x}_{t-1}|\mathbf{x}_t, \mathbf{x}_0)$ :

$$\arg \min_{\theta} \mathcal{D}_{KL}(q(\mathbf{x}_{t-1}|\mathbf{x}_t, \mathbf{x}_0) \| p_\theta(\mathbf{x}_{t-1}|\mathbf{x}_t)) \quad (5)$$

Which, in turn, simplifies to (see Jonathan Ho [2020] for the proof):

$$\arg \min_{\theta} \frac{\bar{\alpha}_{t-1}}{2(1-\bar{\alpha}_{t-1})} \frac{(1-\alpha_t)}{(1-\bar{\alpha}_t)} \| \hat{\mathbf{x}}_\theta(\mathbf{x}_t, t) - \mathbf{x}_0 \|_2^2 \quad (6)$$

In this mathematical framework, optimizing a diffusion model boils down to learn a convolutional neural network  $\hat{x}_\theta$  to predict the original ground-truth image  $\mathbf{x}_0$  from an arbitrarily noisified version of it  $\mathbf{x}_t$  (Luo [2022]).

### 2.3 The Super-Resolution diffusion model (SR3) and its PyTorch implementation

The diffusion model architecture and Pytorch implementation used in this work are based on the work of Chitwan et al. [2021], Patel [2022]. The implementation of Chitwan et al. [2021] is a conditional denoising diffusion model meant to increase the resolution of the input images, for example from  $16 \times 16$  to  $512 \times 512$  pixels. In contrast, Patel [2022] adapted the latter implementation to unconditional satellite image synthesis in order to train a diffusion model on approx. 500000 unlabeled Google Earth Engine screendumps. The PyTorch implementation of Patel [2022] is provided in the github repository DDPM-CD: Denoising Diffusion Probabilistic Models as Feature Extractors for Change Detection. This implementation served as a basis for the training and sampling experiments reported in the result section. The "SR3" model is based on U-Net architecture including a number of residual blocks, up-sampling, drop-out and channel multipliers at different resolutions (Fig. 2). The details of the architecture of the models used in this work are summarized in Table. 1. To grasp the power of satellite image synthesis with generative diffusion model, we experiment sampling on a pre-trained model made of 500M parameters approx. trained on 500000 unlabeled Google Earth Engine screendumps (Chitwan et al. [2021]), which is untractable for GPU-poor ML practitioners. The weights and biases of this pre-trained diffusion model can be downloaded [here](#).

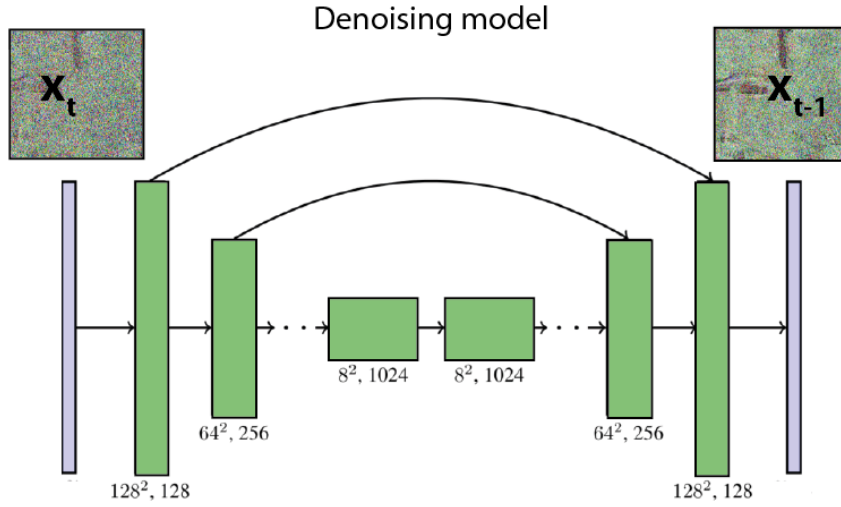


Figure 2: "SR3" super-resolution diffusion model based on U-net architecture from Chitwan et al. [2021]

### 3 Image datasets

#### 3.1 Optical satellite images

The experiments described in this report were conducted using LEVIR-CD256 change detection satellite image dataset from Patel [2022], available for download at <https://www.dropbox.com/scl/fi/r28vh4c6soxk7q9l2hg1a/LEVIR-CD256.zip>. LEVIR-CD256 is of approx. 10000 optical satellite images, made of 3-channels and a resolution of 256 by 256 pixels. They were all collected from Google Earth Engine.

#### 3.2 Handwritten digits

The MNIST dataset <http://yann.lecun.com/exdb/mnist/> is a large collection of handwritten digits commonly used for training and testing in computer vision problems. It contains 60,000 training images and 10,000 test images of digits from 0 to 9, with a resolution of 128 by 128 pixels in grayscale. The dataset serves as a benchmark for evaluating image processing systems and has been pivotal in the development of various neural network and deep learning techniques. In this work, we use a subset of MNIST data (1000 images) to train a denoising diffusion model (section 4.1). We downloaded the MNIST image dataset in png format in Kaggle: <https://www.kaggle.com/datasets/alexanderyyy/mnist-png>.

Table 1: "sr3-type" diffusion model architecture experimented in the framework of this project

| Task          | Channel Dim | Depth Multipliers | # ResNet Blocks | # Parameters | # input images        |
|---------------|-------------|-------------------|-----------------|--------------|-----------------------|
| Training DDPM | 64          | [1, 2, 8]         | 2               | 45M          | 500 MNIST images      |
| Training DDPM | 64          | [1, 2, 4, 8]      | 2               | 55M          | 1000 Satellite images |
| Sampling DDPM | 128         | [1, 2, 4, 8, 8]   | 2               | 391M         | Pre-trained           |

### 4 Results

#### 4.1 MNIST image generation

We trained a "sr3-type" diffusion model (see first line in Table. 1) to generate handwritten digits using 500 MNIST inputs images with 28 by 28 pixels resolution. The training is performed on educloud research machines (Nvidia RTX3090 24GB 24 CPU cores, 64GB RAM). The model training is evaluated on pixel-by-pixel loss metrics based on the generated image and the ground-truth image. We achieved a loss of 4.4841e-03 in approx. 6 hours, with an initial loss of 1e-01. The number of times steps is set to 2000 and the noise (variance) follows a cosine schedule from 1e-06 to 0.01.

On Fig. 3, we show a typical example of sampling the learned model and showing how the denoising is performed along the reverse diffusion chains at various time steps. Qualitatively, we find the digit 7 is adequately generated and easily recognizable. On Fig. 4, nine sampling results are displayed with a varying degree of quality. We find that out of nine generated images, seven digits were easily recognizable.

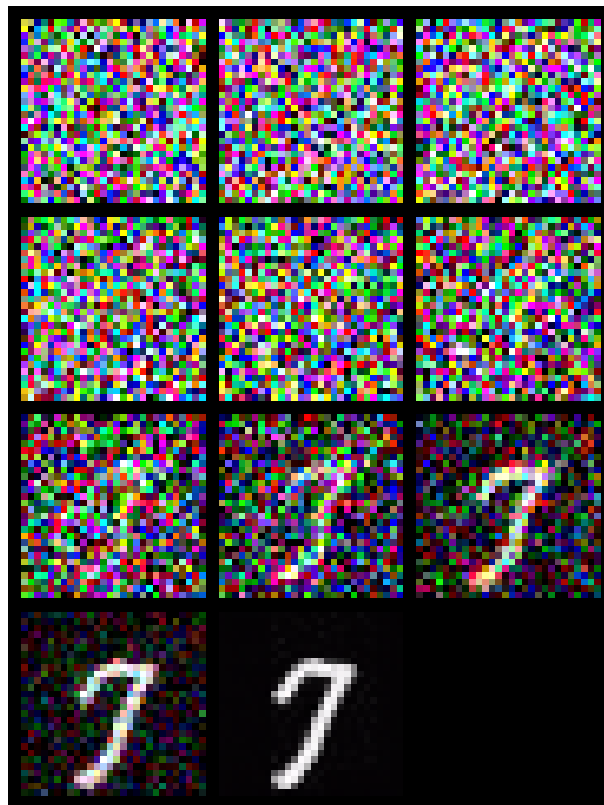


Figure 3: Denoising process from the learned "sr3-type" diffusion model trained on 500 MNIS images

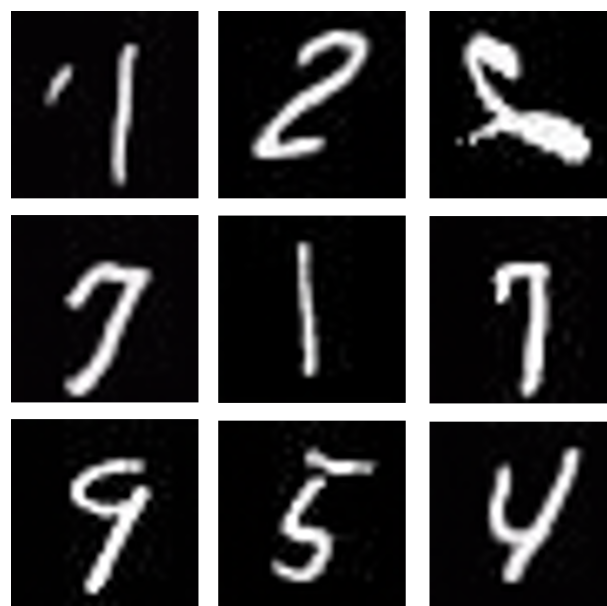


Figure 4: Sampling results showing generated handwritten digits from the learned "sr3-type" diffusion model trained on 500 MNIS images

## 4.2 Satellite image generation

### 4.2.1 Training a diffusion model in 1000 satellite input images

We trained a "sr3-type" diffusion model (see second line in Table. 1) to generate satellite images using 1000 LEVIR-CD inputs images with 256 by 256 pixels resolution. The training is performed on educloud research machines (Nvidia RTX3090 24GB 24 CPU cores, 64GB RAM). For the experiment, we chose to limit the number of inputs images to make the problem tractable for educational purpose. We do expect poor generalization capability but we find that the results allow to grasp the potential of diffusion model for remote-sensing purposes. The model training is evaluated on pixel-by-pixel loss metrics based on the generated image and the ground-truth image. We achieved a loss of 2.0e-03 in approx. 7 hours, with an initial loss of approx. 1. The number of times steps is set to 2000 and the noise (variance) follows a linear schedule from 1e-06 to 0.01.

On Fig. 5, we show a typical example of sampling the learned model and showing how the denoising is performed along the reverse diffusion chains at various time steps. Qualitatively, we find the synthesized image does not seem to represent realistic landscape features. Some lookalike of dirt roads can be observed but they do not form a realistic network as they are abruptly terminated. In the next subsection, we compare the sampling results from the trained diffusion model to 10 times larger diffusion model trained on 100 times larger datasets.

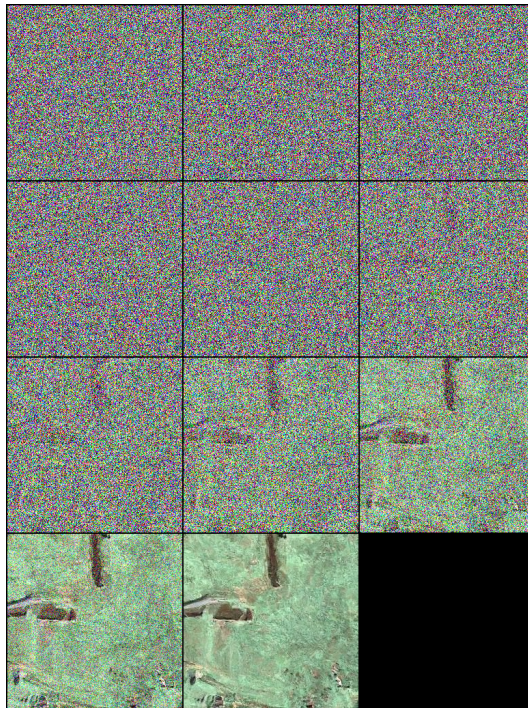


Figure 5: Sampling results from diffusion model trained on 1000 satellite images

### 4.2.2 Sampling a pre-trained model from Patel [2022]

Two synthesized satellite images from the pre-trained diffusion model containing 391M weights and biases (See third line in Table. 1) are displayed in Fig. 5 along with the learned denoising chain of images. Comparing with images generated from trained diffusion model trained in section 4.2.1, the generated satellite images are stunning in both level of details and their variability: urban area with buildings and road infrastructures to forest or field crop areas including seasonal changes (partial snow cover). On the Educloud research nodes (Nvidia RTX3090 24GB 24 CPU cores, 64GB RAM), the sampling process for a single image takes approx. 45 minutes.

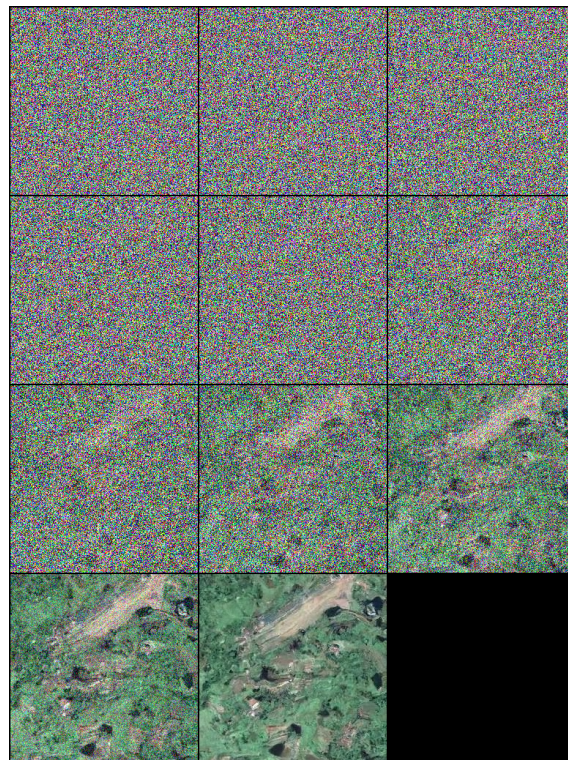
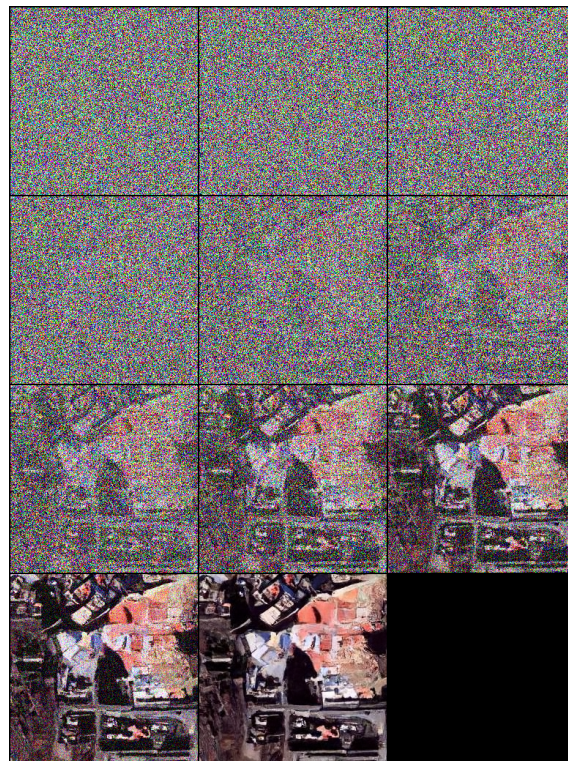


Figure 6: Sampling results from a pre-trained diffusion model from Patel [2022], based on a dataset of 500000 satellite images.

## 5 Discussion and conclusion

### 5.1 Tractability of diffusion models

The results presented in this report confirm the potential of diffusion model for satellite image generation. Sophisticated diffusion models like "sr3" appeared convenient to implement, modify and train in PyTorch. We have adapted the codes to handle handwritten digits and satellite images from the implementation of Patel [2022], Jonathan Ho [2020]. However, we note that the size of diffusion models are consistently very large (ranging from 10M to 100M parameters) and therefore requires GPU-rich computing environments for training. On top of this, for application in remote-sensing and natural sciences, we quickly realize that generalization capability of generative models largely depend on the amount of training images. Gathering 500000 satellite images is not a straightforward process and training a large diffusion models of 390M parameters would weeks on the computer used in this project.

### 5.2 The rise of pre-trained "foundation models"

This work shows that it is practical and easy to use pre-trained diffusion model available open source online. Indeed, such "foundation" models are trained on very large corpus of unlabeled training data and have a great potential for fine-tuning lighter diffusion models, or any downstream tasks on less GPU-intensive learning tasks (Patel [2022]). Such foundations model could help democratize generative models and unleash their increasing power to a larger audience.

### 5.3 Further work

This project deals with satellite image generation with diffusion model but does not investigate the practical applications of diffusion models for Earth Observation data. The potential of diffusion models for change detection in satellite images are great and we could think of important remote-sensing applications like disaster relief (earthquakes, fires) or climate-related (glacier, ice-sheet) monitoring, amongst others. Finally, the amount of open-source satellite imagery is dramatically increasing and are readily available online with tools like Google Earth Engine. We foresee that denoising diffusion probabilistic models will be a tool of choice for analysis of remote-sensing and Earth Observation data. From 2021 and onward, the shift to generative models in the industry has arguably given rise to the "foundation model" paradigm, changing durably the scientific method.

## References

- Pieter Abbeel Jonathan Ho, Ajay Jain. Denoising diffusion probabilistic models. *ArXiv*, 2020. doi:<https://doi.org/10.48550/arXiv.2006.11239>.
- Diederik P. Kingma; and Max Welling. An introduction to variational autoencoders. *arXiv*, 2019. doi:<https://arxiv.org/abs/1906.02691>.
- Prafulla Dhariwal; Alex Nichol. Diffusion models beat gans on image synthesis. *ArXiv*, 2021. doi:<https://arxiv.org/abs/2105.05233>.
- Goodfellow. Generative adversarial network. 2014.
- Thomas Samuel Kuhn. *The Structure of Scientific Revolutions*. 1962.
- Wele Gedara Chaminda Bandara; Nithin Gopalakrishnan Nair; Vishal M. Patel. Ddpm-cd: Denoising diffusion probabilistic models as feature extractors for change detection. *IEEE TRANSACTIONS ON GEOSCIENCE AND REMOTE SENSING*, 2022. doi:<https://arxiv.org/abs/2206.11892>.
- Saharia Chitwan, Ho Jonathan, Chan William, Salimans Tim, Fleet David J., and Norouzi Mohammad. Image super-resolution via iterative refinement. *ArXiv*, 2021. doi:<https://arxiv.org/abs/2104.07636>.
- Calvin Luo. Understanding diffusion models: A unified perspective. *Blog note*, 2022. doi:<https://calvinyluo.com/2022/08/26/diffusion-tutorial.html>.